



Llywodraeth Cymru  
Welsh Government

# 2020-21 Soil Policy Evidence Programme

**Modelling grass growth in  
Wales in the face of a  
changing climate**

02 July 2021

Report code: SPEP2020-21/01



## ADAS General Notes

---

**Project No.:** SPEP2020-21/01

**Title:** Modelling grass growth in Wales in the face of a changing climate

**Client:** Welsh Government; Agricultural Land Use & Soil Policy, Land, Nature and Forestry Division, Department for Rural Affairs

**Date:** 02 July 2021

**Status:** Final

**Authors:** Dr Daniel Hobley, ADAS Bristol, The Old School, Stillhouse Lane, Bristol, BS3 4EB, Dr Steven Anthony, ADAS Wolverhampton, Titan 1 Offices, Coxwell Avenue, Wolverhampton, WV10 9RT, Isabel Corkley, ADAS Wolverhampton, Titan 1 Offices, Coxwell Avenue, Wolverhampton, WV10 9RT, Dr Alison Rollett, ADAS Gleadthorpe, Netherfield Lane, Meden Vale, Nottinghamshire, NG20 9PD and John Williams, ADAS Boxworth, Battlegate Road, Boxworth, Cambridgeshire, CB23 4NN.

**Date:** 02 July 2021

**Technical reviewer:** Isabel Corkley

**Date:** 17 May 2021

**ADAS Project manager:** Alison Rollett

**Date:** 02 July 2021

**Welsh Government Project manager:** Arwel Williams

## EXECUTIVE SUMMARY

---

### Introduction

Wales' countryside is dominated by farmland, with agricultural land covering 90% of the country. Of that farmland, more than 87% of it is given over to either managed grasslands or to rough grazing. Thus, future productivity of this grassland is key to the future of the Welsh farming economy, which produces £1.6 billion in economic output and supports 3.5% of jobs in Wales as of 2019 (Department for Environment, Food & Rural Affairs et al., 2020).

Anthropogenic climate change linked to rising atmospheric CO<sub>2</sub> levels is forecast to alter Welsh climate and weather in ways that will directly affect grass growth. Temperatures are forecast to increase by at least several degrees, winter rainfall to rise by tens of percent, and summer rainfall to fall by tens of percent, with the exact numbers depending on which emissions pathway occurs. The physiology of plants in general and grass specifically is sensitive to all of these changes. Grass depends on soil water supplied by rain to grow, but equally cannot grow in saturated soil. Its growth is slow to zero at low temperatures and is also suppressed at very high temperatures, leaving an optimum temperature window for growth. It is also sensitive to the concentration of CO<sub>2</sub> itself in the atmosphere, with higher concentrations making plants grow faster if all else is equal.

### Approach

**The aim of this scoping project is to quantify the possible effects of climate change on Welsh grassland productivity in the years up to 2080.** It uses a case study approach, estimating changes in productivity at six different farm locations in Wales, covering a wide geographical range and a range of environmental conditions under which grass is grown. A model (the ADAS Grass Model, AGM) that uses weather and soil conditions to project grass growth was used to predict yields of a single representative grass species (ryegrass) at these farms. The model implements seven fixed harvests during the growing season (spring-autumn) in a way that simulates grazing. The project focused on **total yield and seasonality of yield**, both in terms of total dry matter yields but also variability between years.

The model was driven by weather predictions simulated in the most recent UK climate projection data sets (UKCP18 data). These models offer climate projections based on several different emissions scenarios; this study adopted the so-called "business as usual" emissions scenario (RCP8.5). This scenario is pessimistic, but also the most consistent with real emissions trends up to the present day (Schwalm et al., 2020). The model was calibrated to known yield data from farms in or very close to Wales. The model simulated yields across two representative time windows at each of the six sites: 1981-2020 (the modern baseline), and 2041-2080 (the projected window).

Higher CO<sub>2</sub> concentrations increase crop yield independent of its role in driving changes in climate. Hence, the model is sensitive not only to climatic variables, but also – optionally – directly to atmospheric CO<sub>2</sub> concentrations. This feature of the model lets us: 1. isolate the effect of CO<sub>2</sub> fertilisation on changing yields, as set apart from climatic effects, and 2. test for consistency of the modelling method with other approaches that assess relative changes in grassland productivity based on changes in weather alone.

## Key results

### Total yields

The model predicted that climate change had little impact on total dry matter yields **at four of the six sites**. This was due to enhanced growth rates driven by increasing CO<sub>2</sub> concentrations, which compensated for reductions in growth rate due mainly to reduced rainfall. Of the remaining two sites, one experienced an 8% fall in total yield and one experienced a 24% rise (Table ES1).

**Table ES1. Predicted changes in total grass yields as a result of climate change for six sites around Wales.**

Locality	Median yield 1981-2020 (kg/ha)	Median yield 2041-2080 (kg/ha)	Percent change (%)
AngleseyVG	7,000	6,400	-8
AngleseyAvg	8,000	7,900	-1
Trelech	11,000	13,700	24
Wrexham	8,300	8,400	0
Vale	11,900	12,200	3
BuilthWells	13,700	14,100	3

### Seasonality of yields

Despite the apparent resilience of the total yields to climate change, the seasonality of production was profoundly affected (Figure ES1). At all the sites, increases in early season production were predicted. However, **at five out of six sites (all but Trelech), the predictions suggested that there would be a significant reduction grass yields from July onwards, with zero yields predicted in late summer and autumn in some years at several of the sites.**

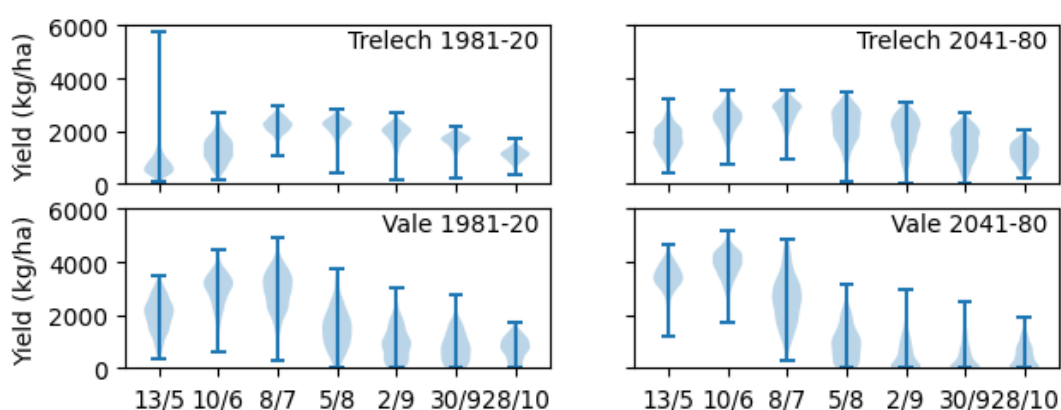


**Figure ES1. Seasonality of yields over the baseline (left) and projected (right) time windows at two indicative sites, Trelech (top) and Vale of Glamorgan (bottom). The bars show full ranges of predicted values, and the shaded areas show the distributions of the most likely values, where the widest point of the shaded area is the most likely value. The remaining four sites are more like Vale than Trelech (see Figure 3.6 in the main report).**

Spring increases in yield reflected both better growth due to cold days being slightly warmer, and also the effect of CO<sub>2</sub> increasing growth rates. The summer falls in productivity were a combined effect of both drought and intense heat suppressing growth, which outweighed any increases in growth due to CO<sub>2</sub> fertilisation effects. These climatic effects were broadly consistent with the predictions of future yield models that use soil types and future changes in weather to forecast relative changes in yields (e.g., Figures Figure 1.1Figure 1.2 in main report).

## Key consequences

Despite total dry matter yields at most of the sites either staying broadly constant or even increasing, the accompanying changes in the seasonality of grass growth was predicted to have major effects on grass utilisation. Grazing animals require feed in the late summer and autumn. If they are to be sustained by the enhanced spring growth, it is likely that the early growth should be converted to silage. This has several consequences:

- Infrastructure and management practices may need to be adapted to allow livestock to be fed with silage in the late summer;
- Using silage as feed may result in different feed quality, which may affect dietary intake;
- Additional costs (e.g. building, feeders, machinery, manure storage etc.) are usually associated with changing from grazed to fed management practices.

These changes may lead to **significant changes to the character and practices of pastoral farming in many places in Wales.**

However, the study suggests that climate change will lead to increased grassland productivity on sites at higher elevations, which currently experience cool, wet weather – similar conditions exist fairly widely over inland western and central Wales. At such sites, major changes may be less likely to be needed.

## CONTENTS

---

<b>1</b>	<b>INTRODUCTION.....</b>	<b>1</b>
1.1	Aims and Objectives of Project .....	6
<b>2</b>	<b>METHODOLOGY.....</b>	<b>8</b>
2.1	Task 1. Data acquisition, processing, and bias correction.....	8
2.1.1	Site selection .....	8
2.1.2	Data selection & processing .....	10
2.2	Tasks 2 & 3. Grass yield modelling with the ADAS Grass Model.....	13
2.2.1	The ADAS Grass Model .....	13
2.2.2	Model calibration.....	15
2.2.3	Model configuration for yield prediction .....	17
<b>3</b>	<b>RESULTS .....</b>	<b>19</b>
3.1	Task 2. Yields with no CO <sub>2</sub> fertilisation. ....	19
3.1.1	Total dry matter yields.....	19
3.1.2	Seasonality of harvest.....	21
3.2	Task 3. Impacts of CO <sub>2</sub> fertilisation on grass dry matter yields.....	25
3.2.1	Total dry matter yields.....	25
3.2.2	Seasonality of harvest.....	26
<b>4</b>	<b>DISCUSSION.....</b>	<b>29</b>
4.1	Which sites prosper?.....	29
4.2	Consequences of changes to seasonality .....	29
4.3	Comparison with categorisation approach .....	30
4.4	CO <sub>2</sub> Fertilisation .....	31
4.5	Further work .....	32
4.5.1	Climate change and management strategies.....	32
4.5.2	Grass quality .....	32
4.5.3	Systematic uncertainties.....	32
<b>5</b>	<b>REFERENCES.....</b>	<b>34</b>



## TABLES

Table 1.1: Probable grass dry matter yields at a range of fertiliser N rates, under different growth classes .....	6
Table 2.1: Study sites for the project .....	9
Table 3.1: Changes in median annual dry matter yield between the study periods for each site (no CO <sub>2</sub> response) .....	21
Table 3.2: Changes in median annual dry matter yield between the study periods for each site (CO <sub>2</sub> -sensitive model) .....	26
Table 4.1: Mean daily temperatures and rainfall amounts for each site .....	29
Table 4.2: Summary of key metrics comparing the RB209 categorization mapping outputs with AGM outputs .....	30

## FIGURES

Figure 1.1: Grass growth classes for Wales under baseline scenario .....	2
Figure 1.2: Grass growth classes in 2080 under UKCP18 high emissions climate scenarios .....	3
Figure 1.3: Summer rainfall totals for Wales under baseline scenario .....	4
Figure 1.4: Soil textures in Wales .....	5
Figure 2.1: Distribution of site locations .....	10
Figure 2.2: GM 20 trial sites used to calibrate the ADAS Grass Model .....	16
Figure 2.3: <i>b</i> parameter calibration values at different fertilization rates for each site .....	17
Figure 3.1: Simulated annual total dry matter yield at six study sites in the 1981-2020 baseline window (no CO <sub>2</sub> response) .....	20
Figure 3.2: Simulated annual total dry matter yield at six study sites in both the 1981-2020 baseline and 2041-2080 projection windows (no CO <sub>2</sub> response) .....	21
Figure 3.3: Simulated dry matter yields across harvests at six study sites (no CO <sub>2</sub> response) .....	23
Figure 3.4: Simulated fraction of total harvest pre-August at six study sites (no CO <sub>2</sub> response) .....	24
Figure 3.5: Simulated total dry matter yield distributions for six sites (CO <sub>2</sub> -sensitive model) .....	25
Figure 3.6: Simulated dry matter yields across harvests at six study sites (CO <sub>2</sub> -sensitive model) .....	27
Figure 3.7: Simulated fraction of total harvest pre-August at six study sites (CO <sub>2</sub> -sensitive model) .....	28

# 1 INTRODUCTION

---

Climate change is forecast to bring substantial changes to the climate of Wales over the next century. These include changes to temperature, rainfall, wind, and sunniness, all in terms of both magnitudes and patterns across the year. Crop growth depends explicitly on these same parameters (e.g., Dellar et al., 2018; Schapendonk et al., 1998; Semenov, 2009; Whiteley et al., 2018), and so continuing climate change in Wales is likely to impact agricultural outputs. Grassland is a key component of Welsh agriculture: 87% of Welsh farmland is grassland or rough grazing ground as of 2020, supporting 9 million sheep and lambs and 1.1 million cattle and calves (Neil, 2020). Consequently it is very important to understand the impact of climate change on grass yields in grazed livestock systems.

Future emissions of CO<sub>2</sub> remain a key uncertainty in modern projections of the magnitudes and effects of climate change. The most recent climate projections for the UK (the Met Office UK Climate Projections, UKCP18; Met Office Hadley Centre, 2018a), in common with other approaches reported by the Intergovernmental Panel on Climate Change (e.g., IPCC, 2014), address this uncertainty by modelling outcomes based on a set of possible emissions scenarios known as the Representative Concentration Pathways (RCPs). The four pathways, RCP2.6, RCP4.5, RCP6, and RCP8.5, are named for the approximate radiative forcing (in W/m<sup>2</sup>) on the atmosphere reached by 2100 and thus are listed here in increasing order of magnitude of climate change. Of these, the RCP8.5 scenario is commonly known as the “business as usual” scenario, representing a future where emissions continue more or less unabated. The most recent data on global emissions reductions indicates that emissions remain on this trajectory (Schwalm et al., 2020).

The weather parameters listed above – temperature, rainfall, wind, and sunniness – are all known to play a key role in agricultural crop yields. However, crops’ responses are not always linear to these variables. Plants tend to grow best within a defined, moderate range of temperatures; both cooler and hotter temperatures will reduce growth rates. In the case of ryegrass, growth more or less stops below 4 °C and above 34-45 °C (Brereton et al., 1996; Romera et al., 2009). Crops require soil moisture to transpire, which is ultimately supplied by rainfall; water stress caused by drier soils will suppress growth (e.g., Christy et al., 2018; Dellar et al., 2018; Hess et al., 2020). However, saturated soils will also inhibit growth (Hess et al., 2020; Laidlaw, 2009). Humidity and vapour pressure also affect transpiration rates (e.g., Kaiser et al., 2015; Monteith, 1965, 1981); in turn, humidity and vapour pressure are also functions of soil moisture and daily temperature range (Allen et al., 1994). Transpiration is also modulated by wind speeds, which move humid air away from the crop’s leaves and replace it with new air (e.g., Allen et al., 1994). Ultimately, the source of energy for plant photosynthesis and thus growth is the intensity of incident solar radiation, and so ambient light and cloudiness are important controls also (Allen et al., 1994; Monteith, 1965, 1981).

Non-weather variables are also important for growth. Soil conditions – e.g., permeability, porosity, depth – are important additional controls on soil moisture. Nutrients available in the soil also play an important role (e.g., Dellar et al., 2018). However, CO<sub>2</sub> levels themselves also control growth rates. CO<sub>2</sub> concentrations affect the biochemical pathways of photosynthesis, and hence also the rates of crop growth (e.g., Kaiser et al., 2015; Rodriguez et al., 1999). This effect is commonly described as “CO<sub>2</sub> fertilisation”, although it is better thought of as an enhancement of plant growth efficiency for given availability of light, water, and nutrients, as opposed to fertilisation in the nutrient sense (Christy et al., 2018).



Distributions of subsets of these key parameters around the UK enable the creation of classification schemes for land suitability for grass crop development. For instance, guidance presented in the AHDB Nutrient Management Guide (RB209) (AHDB, 2021), and ultimately derived from work by Thomas and Young (1990) and Doyle et al. (1986), are used in a separate report by ADAS to the Welsh government under this project to illustrate current and future suitability classes for grass growth around Wales (Hockridge et al., 2020)(Figs. Figure 1.1, Figure 1.2). This approach explicitly prioritises soil moisture as the key parameter controlling growth, and so is based upon summer rainfall (Fig. Figure 1.3) and soil type distributions (Fig. Figure 1.4). It projects widespread, although not uniform, decreases in suitability categories around Wales by 2080, with the extent of the change dependent on the RCP pathway selected (Figs. Figure 1.1, Figure 1.2).

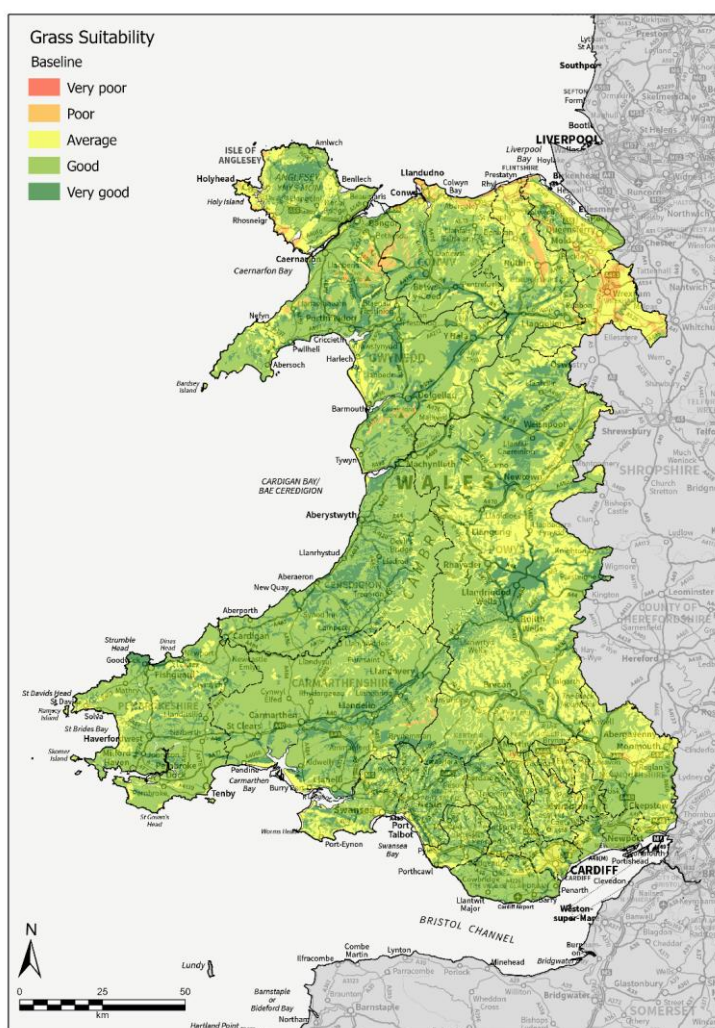


**Figure 1.1: Grass growth classes (very poor, poor, average, good, very good) for Wales under baseline scenario, taken from Hockridge et al. (2020).**

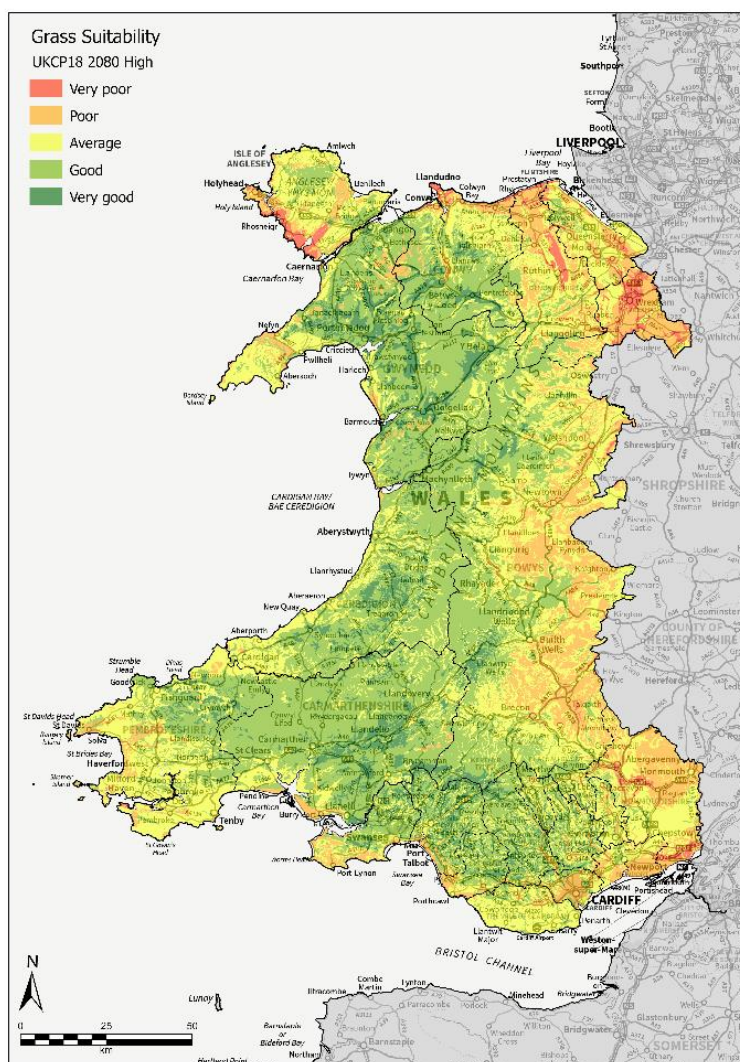


**Figure 1.2: Grass growth classes in 2080 under UKCP18 high emissions climate scenarios, taken from Hockridge et al. (2020).**

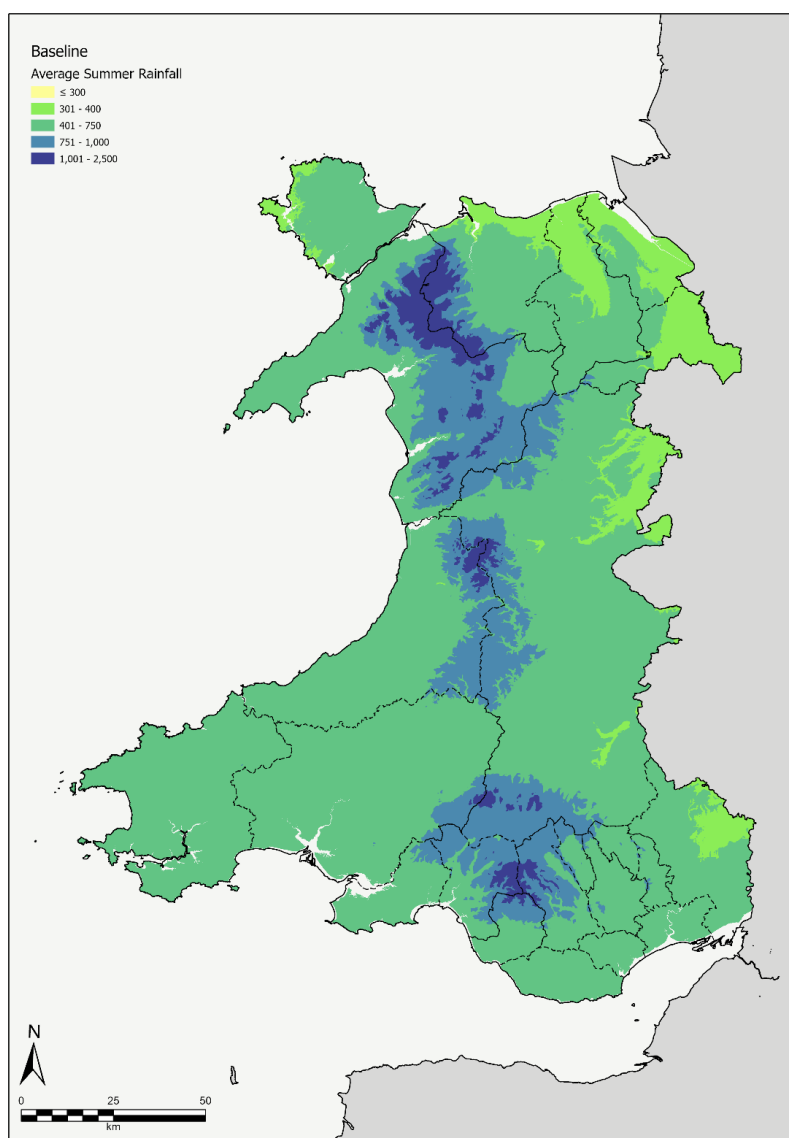


**Figure 1.3: Summer (April-September) rainfall totals for Wales under baseline scenario, taken from Hockridge et al. (2020). Data is drawn from HadUK-Grid (Hollis et al., 2019; Met Office et al., 2018) with a 1961-1990 baseline.**

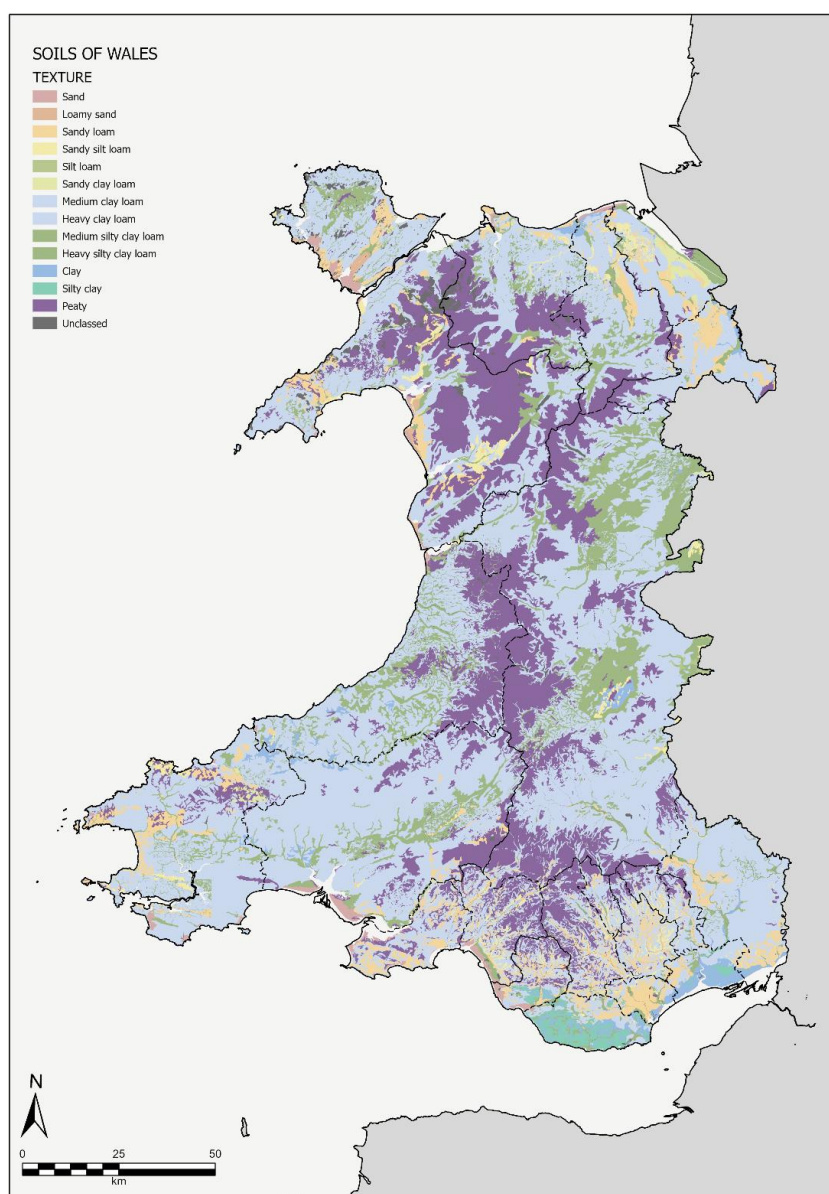


**Figure 1.4: Soil textures in Wales, taken from Hockridge et al. (2020). Underlying data is from Cranfield’s LandIS1 national soil map of Wales.**

Each classification has previously been linked to typical probable annual dry matter yields (Brockman, 1995). These yields vary according to applied nitrogen fertilization rates.

**Table 1.1: Probable grass dry matter yields (t/ha) at a range of fertiliser N rates, under different growth classes. Recommended maximum N rates to apply are also shown. Estimates are for the mid-1980s. Redrawn from Brockman et al. (1995).**

Site class	Fertiliser N application rate (kg/ha)										Maximum to apply (kg/ha)
	0	50	100	150	200	250	300	350	400	450	
Very good	3.2	4.7	6.1	7.5	8.9	10.0	10.9	11.6	12.2	12.7 at	450
Good	2.8	4.2	5.6	7.0	8.3	9.4	10.3	11.0	11.5	11.6 at	410
Average	2.4	3.8	5.1	6.4	7.7	8.7	9.6	10.3	10.5 at		370
Poor	2.0	3.3	4.6	5.9	7.2	8.2	9.1	9.5 at			330
Very poor	1.6	2.9	4.2	5.4	6.6	7.7	8.4 at				300

## 1.1 Aims and Objectives of Project

The aim of the project was to use numerical modelling of grass growth to project changes to the productivity of grazing pastures at sites in Wales, under the influence of a changing climate in the years up to 2080. These changes are to be measured in terms of bulk annual dry matter yield, variability of yield between years, and differences in the seasonality of harvest. Existing studies of crop yield under climate change (e.g., Brereton et al., 1996; Chang et al., 2017; Dellar et al., 2018; Hess et al., 2020; Rodriguez et al., 1999; Semenov, 2009; Whiteley et al., 2018), including as part of this wider study (cf., Hockridge et al., 2020), led to the hypotheses that:

- Likely decreases in summer rainfall in Wales will act to suppress grass growth;
- Likely increases in growing season temperatures will promote growth at lower temperatures but suppress it at higher temperatures (e.g., Brereton et al., 1996; Romera et al., 2009);
- Increased atmospheric concentrations of CO<sub>2</sub> will act to enhance grass growth (“CO<sub>2</sub> fertilisation”)

Through the numerical simulation, this study has quantified the interaction of these three key drivers at different times of the year, and understood their net impact on yield.

The project has not quantified variability of yields across all possible locations in Wales, or across multiple climate scenarios. Instead, the responses at six indicative sites across the country covering a range of possible environmental and climatic conditions have been predicted based on responses to climate change under the RCP8.5 (“business as usual”) climate emissions scenario. The results were based on perennial ryegrass swards under a fixed management regime. Variability in yields at a site were assessed across climatic variations within 4-decade study windows, and across future climate projections from a range of different climate models.

The specific tasks in the project were:

- Acquire time series of climate projections covering the period of study 1981-2080 at six indicative farm sites around Wales. Identify and bias correct two study intervals for each: 1981-2020 (current baseline) and 2041-80 (future projection).



- Use the calibrated ADAS Grass Model (AGM) to predict yields in each window at each site, across seven fixed harvests simulating grazing through the spring and summer, under each climate model realisation. In this objective, the model will *not* simulate CO<sub>2</sub> fertilisation of the grass, and so isolate the climatically driven effects on growth.
- Use the model to predict changes under the same conditions, but this time with CO<sub>2</sub> fertilisation of the grass. Compare the responses in each window to those in the absence of CO<sub>2</sub> fertilisation to isolate its influence on yields and their variability.



## 2 METHODOLOGY

---

### 2.1 Task 1. Data acquisition, processing, and bias correction.

The aim of this task was (i) to acquire climate projection data necessary to run the model, (ii) to process that raw data to give time series of daily weather data at a point in a form calibrated for the model, and (iii) to bias correct the time series in the time intervals of interest. Bias correction ensures that key statistics in those time series are consistent with real weather patterns (e.g., Fung, 2018).

#### 2.1.1 Site selection

Six sites were selected across Wales to examine the potential ryegrass yields. Sites were selected on the following basis:

- Site is currently used for agriculture;
- A range of current yields;
- A range of future yields under existing projections;
- Different soil types and average annual rainfall volumes;
- Spatial coverage.

To establish variability in these classes, the AHDB Nutrient Management Guide (RB209) grass growth productivity guidelines (AHDB, 2021; Thomas & Young, 1990) were mapped as presented in the companion report on this project, “Grass Growth Classes” (Hockridge et al., 2020). This mapping (Figs. Figure 1.1, Figure 1.2, Figure 1.3, Figure 1.4) showed that a large fraction of Wales falls into the “good” bracket both in the baseline and future projection; this reflects high summer rainfall and widespread distribution of soils with medium to high available water capacities on medium or low elevation terrain. Some areas, mainly to the east, fall into the medium summer rainfall categories. These tend to map within the poor or very poor grass growth categories.

Sites were selected based on these maps to encompass variability in grass growing conditions as much as possible. Given the extent of good growth conditions, three sites currently in the Good grass growth category were chosen for the modelling exercise in addition to one each in the very good, average and poor growth classes.

The six sites selected are described in Table 2.1 and mapped in Figure 2.1.

**Table 2.1: Study sites for the project. Classes are derived from mapping in Hockridge et al. (2020). Plant-available soil water content and soil water easily available ratios are derived from the soil type, based on standard values from MAFF's (1988) Agricultural Land Classification of England and Wales.**

Site	Current productivity class	Projected productivity 2080	Soil type	Modern rainfall	Inferred plant-available soil water content (AWC) (mm)	Inferred soil water easily available ratio	Elevation (m)
Trelech	Good	Good	Clay loam	High	150	0.620	196
Vale of Glamorgan	Good	Average	Silty clay	High	141	0.552	59
Builth Wells	Good	Poor	Clay loam	High	150	0.620	232
AngleseyAvg	Average	Poor	Sandy loam	High	147	0.674	102
Wrexham	Poor	Very poor	Sandy loam	Mid	147	0.674	78
AngleseyVG	Very good	Good	Silty clay loam	High	141	0.552	55



**Figure 2.1: Distribution of site locations around Wales. Map boundary shown under ONS, OS OpenData data use agreement.**

### 2.1.2 Data selection & processing

For each site, daily time series of weather data were required to drive the grass growth model. The data had to be available in a consistent and continuous form throughout both selected study windows (1981-2020; 2041-2080).

#### ***Model input data: UKCP18 climate model ensemble***

Through both the baseline (1981-2020) and future prediction (2041-2080) windows, the model was driven with synthetic weather realisations available from the UKCP18 climate modelling project (Met Office Hadley Centre, 2018a). Note that direct observations were not used for the baseline period as direct input into the model because:

- There is a need for consistency and comparability in the form of the data in both windows;
- Spatially resolved, gridded data based on direct observations is only available as monthly averages for some of the key input data;

- Variation in modelling outputs was used as a proxy for variability in possible weather (see below). This would not be possible with only the directly observed weather time series.

The modelled data was part of the UKCP18 national probabilistic climate projection set (Met Office Hadley Centre, 2018a). The regional projections for the UK on a 12km grid, 1980-2080 (Met Office Hadley Centre, 2018b) were used, which contained public sector information licensed under the Open Government License v3.0. This data set provided 12 downscaled projections from the HadREM3-GA705 model, which uses the 60km Hadley Centre global coupled model (GCM) HadGEM3-GC3.05. The 12 different projections represent possible configurations of the Unified Model in that GCM, re-gridded onto the Ordnance Survey's British National Grid. In essence, each of these 12 projections provides a single, coherent possible realisation of daily weather over the duration of the model run (1980-2080), under somewhat different modelling assumptions. All of the realisations in the dataset used the "business-as-usual" RCP8.5 high emissions scenario, and so represent relatively pessimistic climate outcomes.

Of the provided output data from the regional projections, daily gridded model variables were selected that were either directly required by the ADAS Grass Model to run, or needed to derive those driving variables. These model output variables were:

- Maximum daily air temperature, degrees C, "*tasmax*"
- Minimum daily air temperature, degrees C, "*tasmin*"
- Mean daily air temperature, degrees C, "*tas*"
- Precipitation rate, mm/day, "*pr*"
- Net surface short wave radiation flux,  $Wm^{-2}$ , "*rss*"
- Wind speed at 10 m above the surface,  $ms^{-1}$ , "*sfcWind*"

From these daily gridded data, six daily time series at each of the study site localities were extracted using a nearest neighbour algorithm.

#### ***Bias correction: HadUK-Grid gridded observed data***

The climate projection data was used as the basis for driving the ADAS Grass Model. However, the output from such simulations very rarely reproduces the patterns and statistics known to be present in real weather data (e.g., correct means, correct distribution shapes). For this reason, *bias correction* is frequently performed on climate model outputs that are to be used for impact studies such as this project (e.g., Gohar et al., 2017; Hawkins et al., 2013b; Piani et al., 2010; Switanek et al., 2017), and is recommended for use of UKCP18 data (Fung, 2018). Bias correction compares climate model outputs at known locations to observations at those locations, then scales that model output such that selected statistics meet those observed. Bias correction can also reduce error introduced by downscaling of models (including from gridded to point data; Fung, 2018). Multiple methods are available, each seeking to match different sets of statistics, of different complexities, and appropriate to different statistical distributions and use cases. Once calibrated for a use case and for a particular variable in an observed time series, the model's predictions of future climate change may be similarly scaled.

Scaled distribution mapping (SDM) bias correction was applied to each data set (Switanek et al., 2017). SDM is a technique which can account for non-stationarity in error correction values, unlike many other bias correction approaches. Where applied to rainfall data or other parameters which approximate a gamma distribution, it explicitly accounts for the

frequency of rain days and the likelihood of individual events. However, it can also be successfully applied to all of the climate variables considered in this study by specifying that the data are normally distributed. To deploy the SDM correction, the *bias\_correction* v.0.2 Python package was used. This software was developed by and copyright Pankaj Kumar and released under an MIT software license.<sup>1</sup>

The model data were bias corrected against the HadUK-Grid gridded average climate observations for the UK (Hollis et al., 2019; Met Office et al., 2018). HadUK-Grid is a 1km x 1km gridded data product derived from a network of UK land surface observations; in this project data derived from the version of the dataset upscaled to 12km x 12km specifically for comparison with UKCP18 outputs (Met Office et al., 2020) was used. As for the UKCP18 data, a nearest neighbour algorithm was used to derive time series for each of the study sites, for the same set of climate variables.

Unlike the UKCP18 modelled data, daily resolution data were only available for *pr* (rainfall), *tasmin* (minimum temperature), and *tasmax* (maximum temperature) HadUK-Grid data. The remaining parameters were only available at monthly resolution. Where only monthly data was available, bias correction was applied at this scale, although it was possible to work with the daily data once the climate projection dataset as a whole had been rescaled using the monthly averages.

The HadUK-Grid dataset does not provide data for net surface short wave radiation flux (*rss*). Instead, to bias correct the climate model data a time series for *rss* was derived using: (i) the data for monthly sunshine hours from the HadUK-Grid dataset (*sun*); (ii) an estimate of the total extraterrestrial radiation incident on the Earth for a given year and latitude; and (iii) an estimate of day length based on site latitude, longitude, and elevation. We estimated total extraterrestrial radiation following Duffie & Beckman (1980) and Craig (1984), as presented by Allen et al. (1994):

$$R_a = \frac{24 \times 60}{\pi} G_{sc} d_r (\omega_s \sin \varphi \sin \delta + \cos \varphi \cos \delta \sin \omega_s) \quad (2.1)$$

where  $R_a$  is total extraterrestrial radiation ( $\text{MJ m}^{-2} \text{d}^{-1}$ ),  $G_{sc}$  is the solar constant ( $0.0820 \text{ MJ m}^{-2} \text{min}^{-1}$ ),  $d_r$  is the relative Earth-Sun distance,  $\delta$  the solar declination (rad),  $\varphi$  the latitude (rad), and  $\omega_s$  the sunset hour angle, and

$$\omega_s = \arccos(-\tan \varphi \tan \delta) \quad (2.2)$$

$$d_r = 1 + 0.033 \cos\left(\frac{2\pi}{365} J\right) \quad (2.3)$$

where  $J$  is the Julian day. We estimated the sum of day length for all days in a month,  $n_{mon}$ , with the *astral* v.2.2 Python package. This software was developed by and copyright Simon

---

<sup>1</sup> [https://github.com/pankajkarman/bias\\_correction](https://github.com/pankajkarman/bias_correction)

Kennedy and released under an Apache 2.0 software license.<sup>2</sup> With these parameters, net shortwave incident radiation received by the crop canopy,  $R_{ns}$ , was calculated following Allen et al. (1994) as:

$$R_{ns} = (1 - A) \left( 0.25 + 0.50 \frac{n_{sun}}{n_{mon}} \right) R_a \quad (2.4)$$

where  $A$  is the albedo of the crop (here taking the reference value for grass, 0.23), and  $n_{sun}$  is the total bright sunshine hours each month, which is taken as the *sun* variable in the HadUK-Grid dataset.

### **Recalculation and padding of variables**

In most cases the variables provided from the UKCP18 climate simulations were appropriate to directly drive the ADAS Grass Model, after some unit conversion. However, this was not the case for the wind speed parameter,  $U$ , which in the grass model is calibrated at 2 m above ground level, but in the UKCP18 output is described at 10 m above ground level. We performed the necessary correction following Allen et al. (1989) as shown in Allen et al. (1994):

$$U_2 = U_{10} \frac{4.87}{\ln(67.8z_m - 5.42)} \quad (2.5)$$

where  $U_2$  is the mean windspeed at height 2 m,  $U_{10}$  is the mean windspeed measurement at height 10 m, and the observation height,  $z_m = 10$  m. This approach assumes a standardised reference crop with height 0.12 m, and a roughness parameter for momentum over the crop of 0.015.

UKCP18 climate simulations assume a year is constructed of 12 fixed duration, 30-day months. However, the ADAS Grass Model requires standard observed weather variables for each day in a year, and so expects 365-day years (or 366 in a leap year). To create “normal” duration years, we adjusted the UKCP18 output time series by adding extra days into the 360 day sequence at what would be the ends of January, July, August, October, and December, also adding end of May in the case of a leap year. These days were duplicates of the preceding days.

## **2.2 Tasks 2 & 3. Grass yield modelling with the ADAS Grass Model.**

### **2.2.1 The ADAS Grass Model**

This project used the ADAS Grass Model (Whiteley et al., 2018) to simulate ryegrass crop development and dry matter harvest yields for each site. A variety of other models are available which also simulate grass crop growth under imposed climate conditions (e.g., Chang et al., 2017; Hawkins et al., 2013a; Rodriguez et al., 1999; Romera et al., 2010;

---

<sup>2</sup> <https://github.com/sffjunkie/astral>



Schapendonk et al., 1998; Watson et al., 2015); however, the ADAS model was selected for this project as it was developed specifically to simulate UK conditions, and also because it can be and has been successfully calibrated for specific local field sites where harvest data are available (see below).

The ADAS Grass Model (AGM) is based on the PGSUS grass model of Romera et al. (2010), adapted for UK conditions (the PGSUS model was originally designed to simulate ryegrass pasture growth in New Zealand). The AGM is implemented in Excel with VBA bindings for automated input and output of bulk data. The model equations are described in full in an index within the model spreadsheet, but key functionality and differences from PGSUS described briefly below.

At the core of both models is mass balance between new green growth added to the biomass pool, and green biomass removal by senescence of herbage and harvesting. However, the AGM implements explicit tracking of both the green and senesced biomass pools (following a predecessor model to PGSUS; McCall & Bishop-Hurley, 2003), whereas PGSUS only tracks the green biomass pool. Growth in both models is a function of incident solar radiation, an efficiency term that describes photosynthesis rates per unit solar radiation, a green canopy light interception term, a suppression factor related to water stress in the soil, a maintenance respiration parameter that must be supplied before growth can proceed, and a temperature growth factor which partially or fully inhibits growth over certain temperature ranges. The AGM adopts a function describing change in the growth factor with temperature which follows a recalibrated version of the relationship given by Brereton et al. (1996) rather than that adopted by Romera et al. (2010), on the basis that the Brereton calibration is more applicable to UK crop and conditions. The Brereton relationship gives slower increases in growth rates at lower temperatures and earlier onset of growth suppression at higher temperatures (>25 °C), but both relationships are essentially the same shape, predicting no growth below 4 °C, a peak in growth around 20-25 °C, and falling growth rates above that window. No growth is possible in the AGM above 40 °C. This leads to the key growth equation:

$$N = 10(\alpha I g_T g_W c(G) - r(G)) \quad (2.6)$$

where  $N$  is the new green growth (kg dry matter/day),  $\alpha$  is a scaling factor for growth rate under given incident radiation,  $I$  is the incident solar radiation ( $\text{MJm}^{-2}\text{d}^{-1}$ ),  $g_T$  is a scaling factor for temperature effects,  $g_W$  is a scaling factor for soil water,  $c(G)$  is a scaling factor for green canopy light interception capability, and  $r(G)$  is the daily maintenance respiration ( $\text{g DM m}^{-2} \text{d}^{-1}$ ).

Following PGSUS, the AGM implements an evapotranspiration model that couples crop, groundwater, and atmosphere. The crop draws on groundwater and transpires that moisture; the rates at which both processes occur depend on the soil moisture conditions and aerodynamic roughness of the crop respectively. Soil moisture responds to evapotranspiration rates and replenishment by rainfall, and may saturate. Soil properties in part control the soil water dynamics, and can be calibrated (see below). Representative soil property values for each soil texture and class were derived from published tables (MAFF, 1988) (see also Table 2.1).

The model exposes two calibratable parameters,  $a$  and  $b$ , that control the amount of crop growth for given light conditions ( $\alpha$ ):

$$\alpha = \frac{b}{1 - \exp(-aI)} \quad (2.7)$$

Here  $a$  reflects seasonality in the response and  $b$  controls the absolute magnitude of the growth achieved (Whiteley et al., 2018). These parameters implicitly incorporate the effects of fertiliser use on the crop, i.e., a better fertilised crop receives a higher value of  $b$ . In this way, it is possible to specify the manufactured nitrogen fertiliser application rate in the AGM.

This version of the AGM implements an optional routine to simulate fertilisation of the crop by atmospheric CO<sub>2</sub> concentrations in a simple way. Existing work on cropland productivity under an evolving climate indicates that this effect is nontrivial and important in understanding the magnitude of any changes to harvests (e.g., Chang et al., 2017; Dellar et al., 2018; Semenov, 2009), and so it is important to consider its effect in this study. These adjustments are present in neither PGSUS nor the earlier version of the AGM. Instead, the approach taken in current versions of the LINGRA grass pasture model (Rodriguez et al., 1999; Schapendonk et al., 1998; Wolf, 2006) was adopted in this study. If activated in the model, growth rates in the absence of other stressors increase logarithmically with increasing CO<sub>2</sub> concentrations (Whiteley et al., 2018; Wolf, 2006), which leads to a modified version on Equation (2.6):

$$N = 10(\alpha I g_{CO_2} g_T g_W c(G) - r(G))$$

if CO<sub>2</sub> fertilisation active:  $g_{CO_2} = 1 + 0.8 \log\left(\frac{C_{CO_2}}{360}\right)$   
else:  $g_{CO_2} = 1$

(2.8)

where  $g_{CO_2}$  is a scaling factor for CO<sub>2</sub> concentration and  $C_{CO_2}$  is the atmospheric concentration of CO<sub>2</sub> (ppm). This implementation of CO<sub>2</sub> sensitivity is relatively simple, and could potentially be significantly enhanced to reflect more details of grass physiology (cf., Rodriguez et al., 1999). Note in particular that there is no interaction of CO<sub>2</sub> fertilisation with drought stress or N-limitation, no consideration of interaction with plant energy stores or transitions to and from vegetative growth/flowering, and no consideration of possible concomitant changes in plant water use efficiency as the climate changes (cf., Rodriguez et al., 1999). These effects are considered further in the Discussion (Section 4).

## 2.2.2 Model calibration

### *Growth rates and fertilisation*

The original use of the AGM was for a study (Whiteley et al., 2018) that sought to reproduce grassland productivity across the UK at sites that were part of the “GM 20” trials performed by ADAS & GRI in the 1970s (Morrison et al., 1980). These trials focused on understanding yield responses of grassland under different nitrogen fertiliser regimes. As such, the AGM is already calibrated for various sites around the UK, and the way that N fertiliser use affects the key rate scaling parameters  $a$  and  $b$  is well understood. The model was calibrated using known soil parameters at each site.

The scaling adopted for this study was the mean of the four GM 20 sites that were either in or very close to Wales (Figs. Figure 2.1, Figure 2.2). The value of  $a$  is fixed as the national mean, then the value of  $b$  is calibrated for each site individually using the GRG Nonlinear solving method in Microsoft Excel Solver to minimize the sum of squares of differences between observed and fitted grass yields (Whiteley et al., 2018).

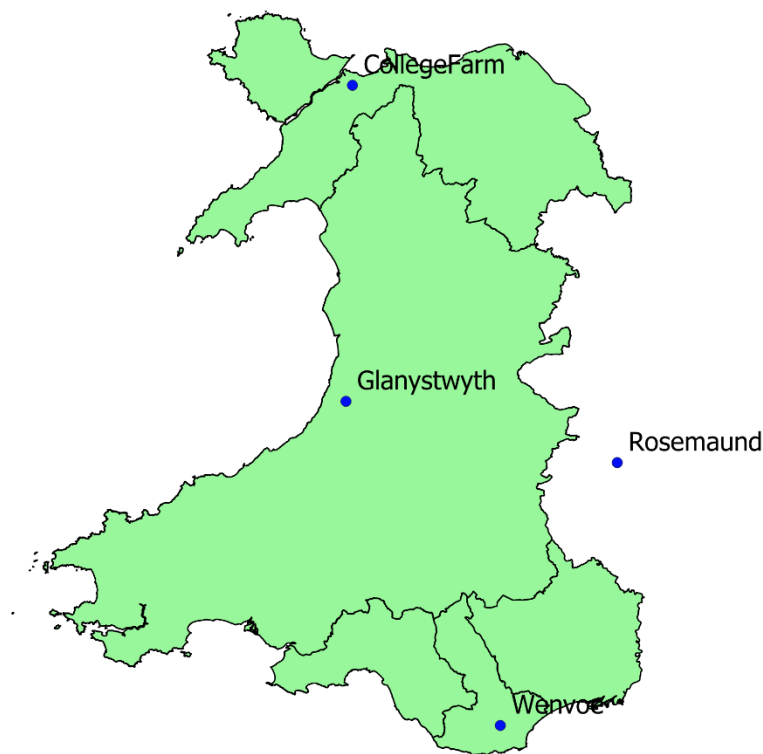


**Figure 2.2: GM 20 trial sites used to calibrate the ADAS Grass Model for this study. Boundaries are shown under an ONS, OS OpenData agreement.**

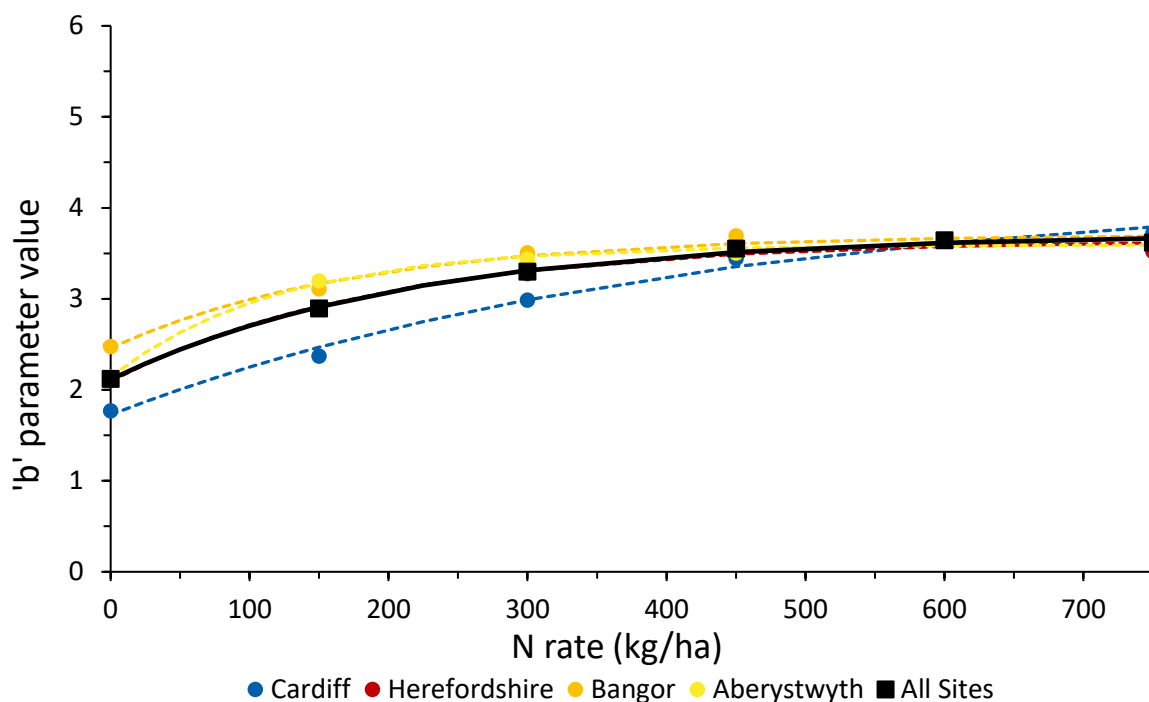


**Figure 2.3: *b* parameter calibration values at different fertilisation rates for each site, under an imposed national mean value of *a* (=0.2616). The sites are Wenvoe (Cardiff), Rosemaund (Herefordshire), College Farm (Bangor), and Glanystwyth (Aberystwyth).**

### 2.2.3 Model configuration for yield prediction

The harvests within the model were configured as simulated grazing. Seven harvest events were simulated for each year, spaced by four weeks and fixed on 13/05, 10/06, 08/07, 05/08, 02/09, 30/09, and 28/10. Each cut reduced the total biomass back to 1200 kg/ha; if less biomass than this was present, no cut was made.

Values of the *a* and *b* growth rate parameters were selected to mimic nitrogen applications of 150 kg N/ha/y (Figure 2.3). This amount of fertilization is consistent with Brockman's (1995) guidelines (see Table 1.1), and would be expected to produce c.10 t/ha dry matter based on RB209 Guidance.

The calibrated model was automated to run for each of the six simulation sites through the 100 years of daily UKCP18 climate realisation data, once for each of the 12 possible UKCP18 climate model configurations. For each simulation, the two windows of interest, 1981-2020 (baseline) and 2041-2080 (projection) were extracted. Each year comprised seven individual harvests. For each studied time window, the response of six sites was modelled, generating 12 x 40 = 480 simulations of sequences of seven harvests. Statistics were then derived for this total population of simulations for each site for each window. As noted previously, this approach sought to understand the average climate across each window, and used each year as a different possible realisation of the weather within a relatively constant climate across 40 years. For each year of data, the model was run twice consecutively on the same input data, i.e., as if two identical years occurred one after the other, and the results were drawn

from the second of these repeated years. This approach removes artifacts in the results related to the arbitrary initial conditions supplied to the model at the start of each model run.

We used these sets of 480 simulations to understand the distributions of total dry matter yield and seasonality of yield in both the baseline and future time periods, both in the absence (Task 2) and presence (Task 3) of CO<sub>2</sub> fertilisation of the crop.

## 3 RESULTS

---

### 3.1 Task 2. Yields with no CO<sub>2</sub> fertilisation.

#### 3.1.1 Total dry matter yields

We derived bulk annual dry matter yields for the six sites by summing the total from each of the seven harvests.

##### *1981-2020*

Yields from the six sites exhibited significant modelled variation in total yield in the baseline window (Figure 3.1). The modelled yields are likely to be theoretical maximum harvests, since the model does not capture limiting factors such as pests or disease, or other chance interventions or disruptions to the crop. Predicted median harvests ranged from 6.5 to 12.8 t/ha (see also Table 3.1). This range of 6.3 t/ha is comparable to the total variability in modelled yields between years in the most productive localities, Builth Wells and Vale of Glamorgan.

The inter-year variability between sites (i.e., the slope of the line of the CDF) was in general comparable. The notable exception was the wettest and coolest site, Trelech, where there was less variability around the median yield.

The baseline total median dry matter yields were sometimes higher than those suggested by Brockman (1995) for similarly fertilized fields (Table 1.1), reflecting differences between the two approaches. The AGM models best possible yields under given conditions, ignoring the effects of pests, disease, and other local issues with production. Also, the baseline estimates extend to 2020, decades after the early 1980s period considered by Brockman (1995), and the yield estimates presented by Brockman are conservative, commonly representing the 30<sup>th</sup> percentile of the distribution, rather than the median dry matter yield (cf., Thomas & Young, 1990).



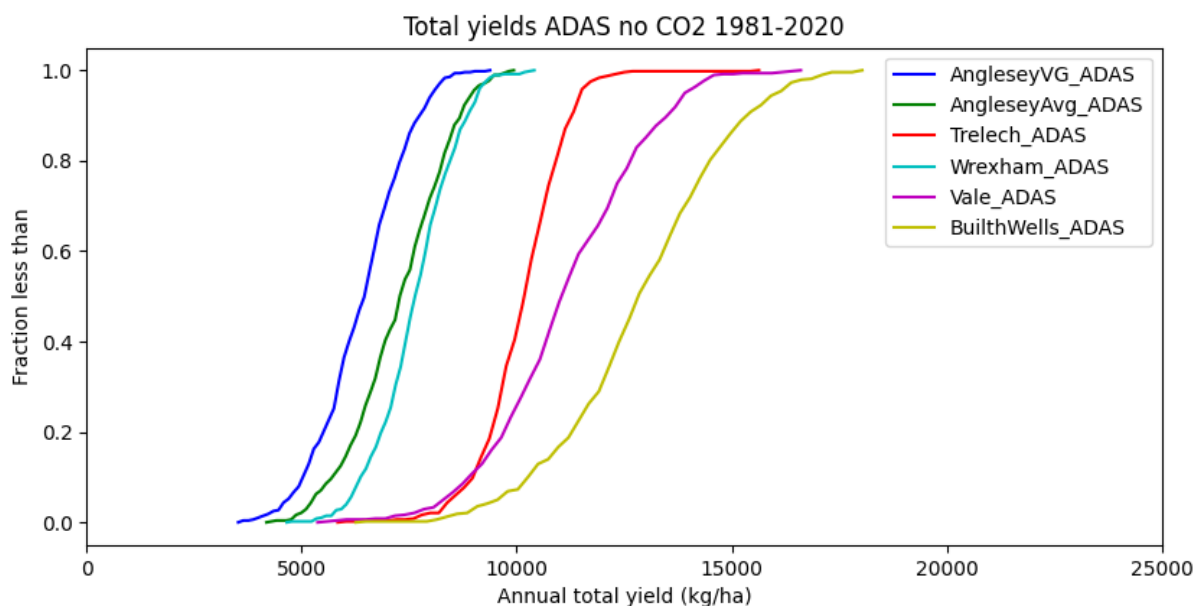


**Figure 3.1: Distributions of simulated annual dry matter total harvest at six study sites in the 1981-2020 baseline window, presented as cumulative distribution functions. Distributions comprise 40 individual years calculated across 12 model variants.**

### 2041-2080

The AGM with no CO<sub>2</sub> fertilisation predicted a reduction in median yield for all six sites in the 2041-2080 window (Figure 3.2, Table 3.1) compared with the 1981-2020 window. The reduction varied between sites, ranging from small (2%, at Trelech) to significant (30%, at one of the Anglesey sites). In general, the pattern was a systematic downward shift in the distributions of total yield; however, the variability at all of the sites also increased slightly (i.e., the gradients on the graphs are slightly lower). This was most obvious for the Trelech and Wrexham sites. At Trelech, the increase in variability meant that although the median yield fell slightly, in around 30% of the simulations yields increased. At Wrexham, the increase in variability is most obvious in the marked collapse of yield in around 20% of the simulations.

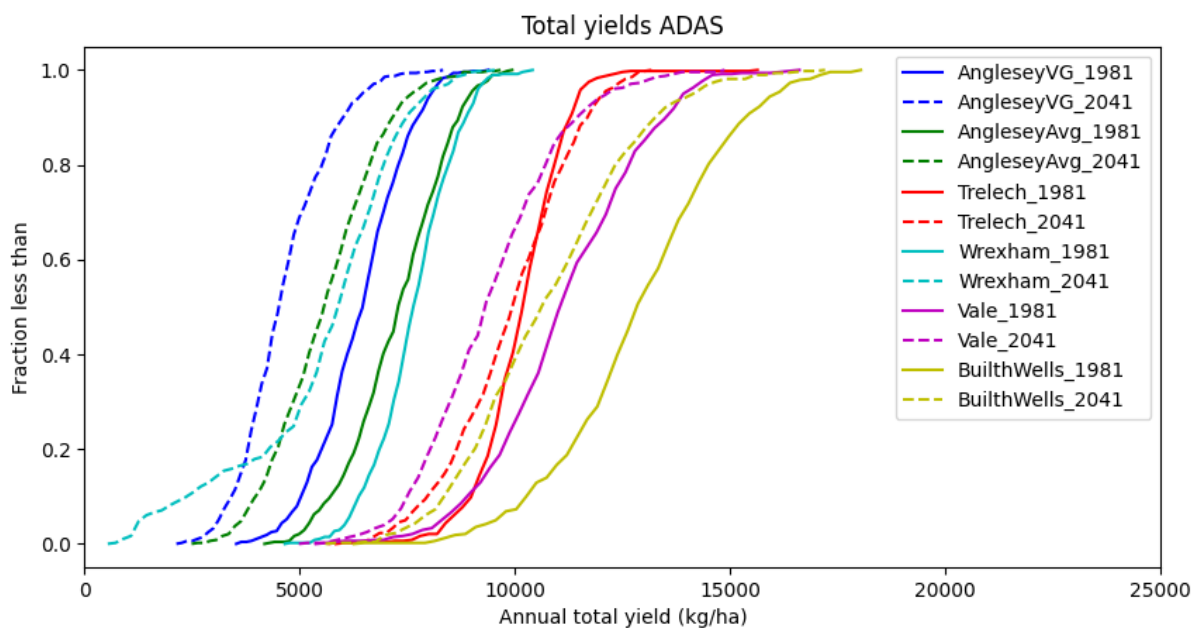


**Figure 3.2: Distributions of simulated annual dry matter total harvest at six study sites in both the 1981-2020 baseline (solid lines) and 2041-2080 projection (dashed lines) windows, presented as cumulative distribution functions. Distributions comprise 40 individual years calculated across 12 model variants.**

**Table 3.1: Changes in median annual dry matter yield between the study periods for each modelled site, for the model without CO<sub>2</sub> fertilisation.**

Locality	Median yield 1981-2020 (kg/ha)	Median yield 2041-2080 (kg/ha)	Percent change (%)
AngleseyVG	6,500	4,500	-30
AngleseyAvg	7,300	5,600	-24
Trelech	10,200	9,900	-2
Wrexham	7,600	5,900	-23
Vale	11,000	9,300	-16
BuilthWells	12,800	10,600	-17

### 3.1.2 Seasonality of harvest

The seasonality of dry matter yield through the year (Figure 3.3) helps to explain the changes seen in total yields. In the 1981-2020 baseline window, there was a common pattern for all six sites – moderate yields in spring rising to a peak in early July, followed in most cases by a gradual decline in yield through the later part of the year. At all sites, median harvests in late September and October were small but non-zero. The decline in harvests after the July peak

was faster at some sites than others: Trelech had a slow decline, whereas the Vale of Glamorgan was predicted to decrease the fastest.

In the 2041-2080 projection window, the patterns in dry matter yield changed markedly. In the early part of the year (first two harvests), yields were predicted to increase significantly above the 1981-2020 baseline. The third, early July harvest was broadly equivalent to the baseline in many years, but a marked decrease was predicted in some years. This lowered the median dry matter yield for July compared to the baseline. This shifted the period of peak production from early July to early-mid June at five of the six sites.

From the August harvest onwards, median yields at all sites were predicted to be lower than the baseline. At the best performing sites (Trelech, Builth Wells), this was expressed as a significant broadening of the predicted yield distributions to lower values, reflecting many years with significant yield reductions. However, at other sites, the downward shift in the distribution was more severe: the median yield was predicted to reduce to zero for harvests in September and October, and at three of these four sites, the median for August was also very close to zero.

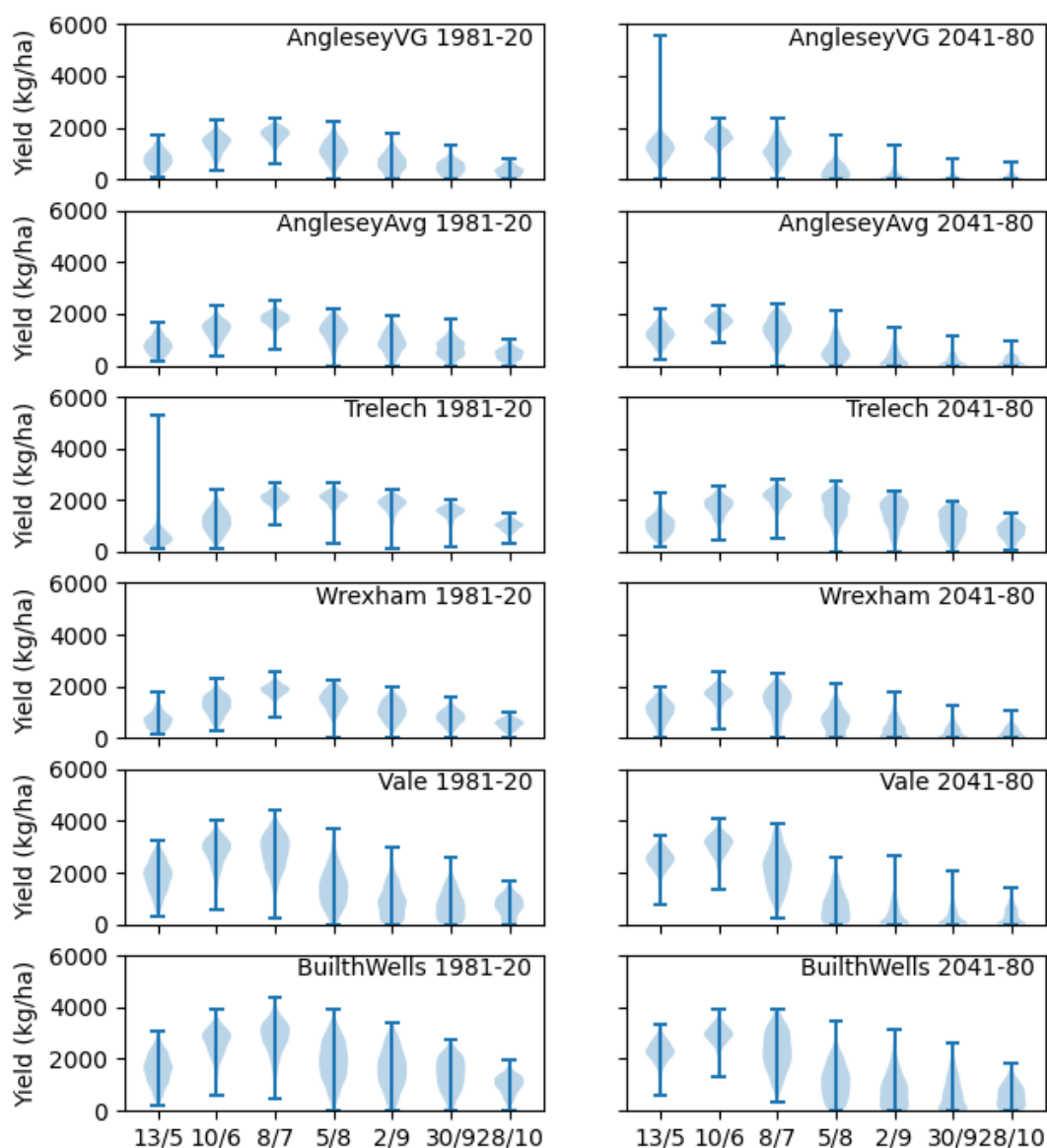


**Figure 3.3: Violin plots of simulated dry matter yields in each harvest at six study sites, for the 1981-2020 baseline window (left) and the 2041-2080 projection window (right) in the model without CO<sub>2</sub> response. Bars represent the range of the data, and the shaded areas represent the shape of the distributions of the data for each harvest. Distributions comprise 40 individual years calculated across 12 model variants.**

Cumulative distribution functions of the proportion of the harvest collected before August provide an alternative method for visualizing differences in yield patterns for both the baseline and projected windows (Figure 3.4). In all cases, a substantial upward shift in this fraction was observed in the later window, with the median fraction increasing between ~0.1 and ~0.3 points. Notably, for the 2041-2080 interval, all sites but Trelech and Builth Wells were predicted to yield no grass at all in or after August in some years. Again, Trelech was the best performing site by this metric by some margin.

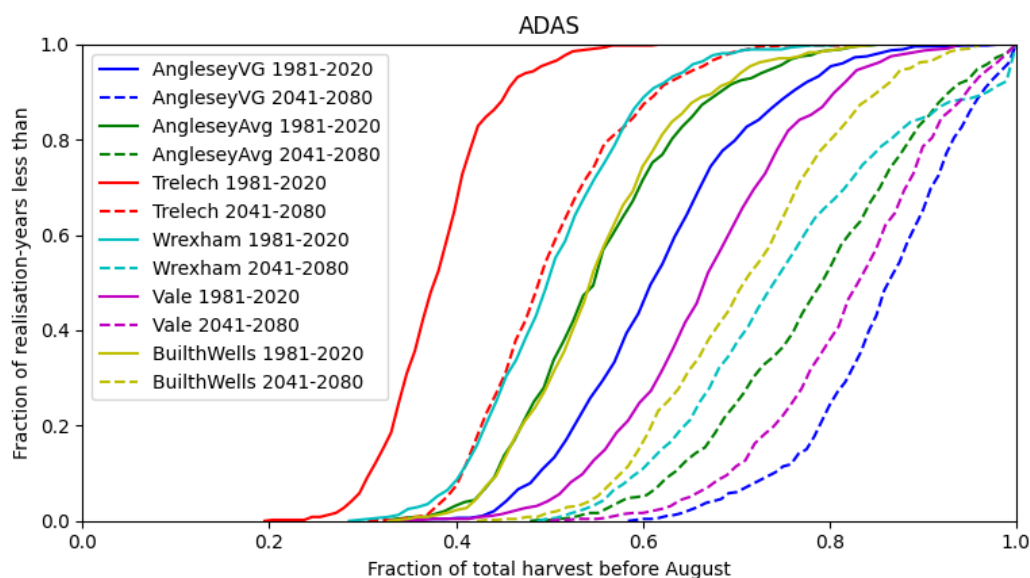


**Figure 3.4: Distributions of simulated fraction of total harvest pre-August at six study sites in both the 1981-2020 baseline (solid lines) and 2041-2080 projection (dashed lines) windows, presented as cumulative distribution functions. Distributions comprise 40 individual years calculated across 12 model variants.**

Examination of the model outputs, and in particular the responses of the various  $g$  scaling parameters in Equation (2.8) as the models evolve, enabled some qualitative understanding of the harvest dynamics documented above. In spring in the projected window, the crops were predicted to experience slightly higher temperatures than the baseline, and have access to adequate soil moisture. The moisture content reflects the combined effects of excess winter rainfall replenishing soil moisture deficit from the previous growing season and spring rainfall recharging the soil water, followed by only moderate evapotranspiration resulting from moderate early season temperatures. However, in the late summer, the combined effects of predicted increased temperatures and reduced summer rainfall in the future scenario stress the crop. At high temperatures  $g_T$  falls rather than rises with increasing temperature, acting by itself to reduce growth. The predicted decrease in rainfall and increase in heat-accelerated evapotranspiration lead to concurrent reductions in  $g_w$  (i.e., drought). Synchronous summer decreases in both  $g_T$  and  $g_w$  result in a marked decrease in predicted grass productivity, although the predicted yield response was dominated by changes in  $g_w$ , the soil moisture term. The temperature-driven spring yield increases were not predicted to compensate for these summer yield reductions, and so the total yields fall in a typical year.

These controls on productivity also explain the strong performance of Trelech in terms of its total yields. Trelech is at high elevation (196 m; Table 2.1), which reduces air temperature, and its position in south west Wales is reflected in high average annual rainfall. These properties limit the heat and drought stresses that begin in August at the other sites.

## 3.2 Task 3. Impacts of CO<sub>2</sub> fertilisation on grass dry matter yields.

To isolate the effect of CO<sub>2</sub> fertilisation on grass dry matter yields, the modelling exercise was repeated using the AGM with the CO<sub>2</sub> sensitivity included.

### 3.2.1 Total dry matter yields

Addition of CO<sub>2</sub> fertilisation to the model had a marked effect on total grass dry matter yield predictions (Figure 3.5, Table 3.2). Harvests were predicted to be ~5-10% higher than the no-CO<sub>2</sub> equivalents in the 1981-2020 baseline period, which is an artifact of the way the model was calibrated using 1970s data. However, comparing the 2041-2080 windows before and after CO<sub>2</sub> inclusion showed significant increases in predicted yields of c.20 percentage points for all sites in all years when CO<sub>2</sub> was included. This is demonstrated in Figure 3.5 by the broadly parallel, rightward shifts of the cumulative distribution functions for the 2041-2080 window (dashed lines) after CO<sub>2</sub> inclusion (see also Tables Table 3.1, Table 3.2). This 20% enhancement in yield due to CO<sub>2</sub> fertilisation is comparable to values reported elsewhere in the literature (Dellar et al., 2018), including from other numerical models (e.g., Rodriguez et al., 1999). The upward shift in productivity means that the CO<sub>2</sub> fertilised model is predicting **total yields that are broadly unchanged from the baseline window predictions** in four of our six sites. The poorest-performing site (AngleseyVG) was predicted to experience only an 8% reduction in total yield; the best-performing site (Trelech) was predicted to experience a substantial (24%) *increase* in dry matter yields.

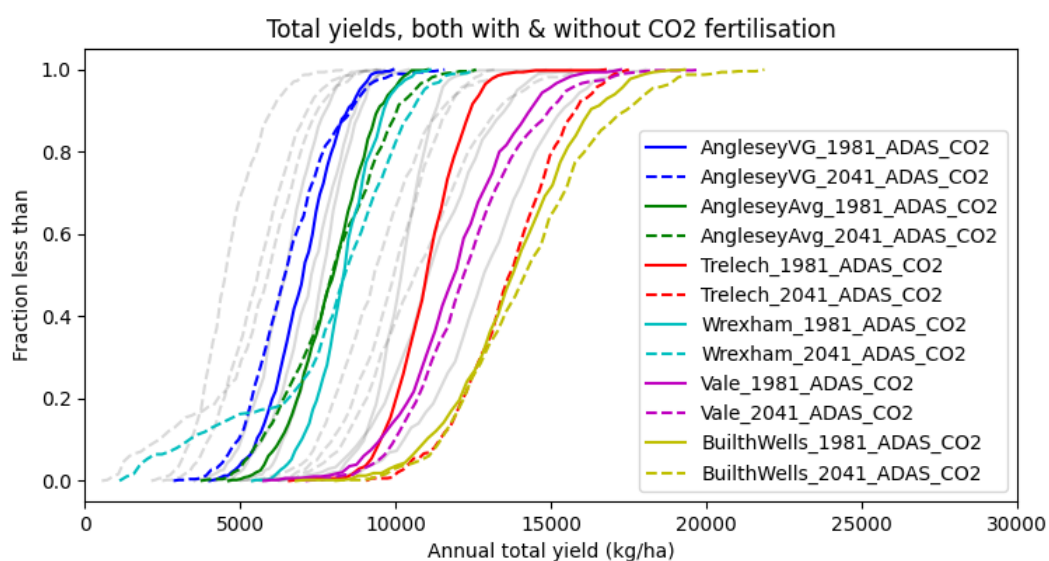


**Figure 3.5: Total dry matter yield distributions for the six sites from the CO<sub>2</sub>-sensitive version of the AGM. Solid lines are baseline window; dashed projected window. The model outputs from the CO<sub>2</sub>-insensitive model, identical to those in Figure 3.2, are shown in greyscale for comparison. Distributions comprise 40 individual years calculated across 12 model variants.**

**Table 3.2: Changes in median annual dry matter yield between the study periods for each modelled site, under the model with CO<sub>2</sub> fertilisation (cf. Table 3.1).**

Locality	Median yield 1981-2020 (kg/ha)	Median yield 2041-2080 (kg/ha)	Percent change (%)
AngleseyVG	7,000	6,400	-8
AngleseyAvg	8,000	7,900	-1
Trelech	11,000	13,700	24
Wrexham	8,300	8,400	0
Vale	11,900	12,200	3
BuilthWells	13,700	14,100	3

The variability in the predicted baseline yield distribution was similar to the no-CO<sub>2</sub> case, and variability of predicted yields for the future scenario also increased slightly, as it did in Section 3.1.1. The ordering of the sites according to median yield productivity was also the same as the no-CO<sub>2</sub> scenario, in both windows (AngleseyVG-AngleseyAvg-Wrexham-Trelech-Vale-BuilthWells in 1981-2020; AngleseyVG-AngleseyAvg-Wrexham-Vale-Trelech-BuilthWells in 2041-2080).

### 3.2.2 Seasonality of harvest

There were few differences in the seasonality of growth when comparing the baseline window predictions from the two CO<sub>2</sub> scenarios of the model (Figs. Figure 3.3, Figure 3.6). In the 2041-2080 projected window, the form of the distribution was largely unchanged from the CO<sub>2</sub>-unfertilised equivalent, with most sites still showing **a rise in yield up to the end of June, a decline into July, followed by an abrupt decrease in productivity from August onwards**. However, dry matter yields all increased compared to the non-CO<sub>2</sub> scenario. Generally, the predicted increases were small in absolute terms in the late season, but in the early season they added significantly to total yields. It is this effect that accounts for the apparent maintenance of total yield for many sites under the CO<sub>2</sub>-sensitive model (Figure 3.5; Table 3.2). With CO<sub>2</sub> fertilisation, the predicted early season growth boost *is* now able to compensate for the late season collapse.



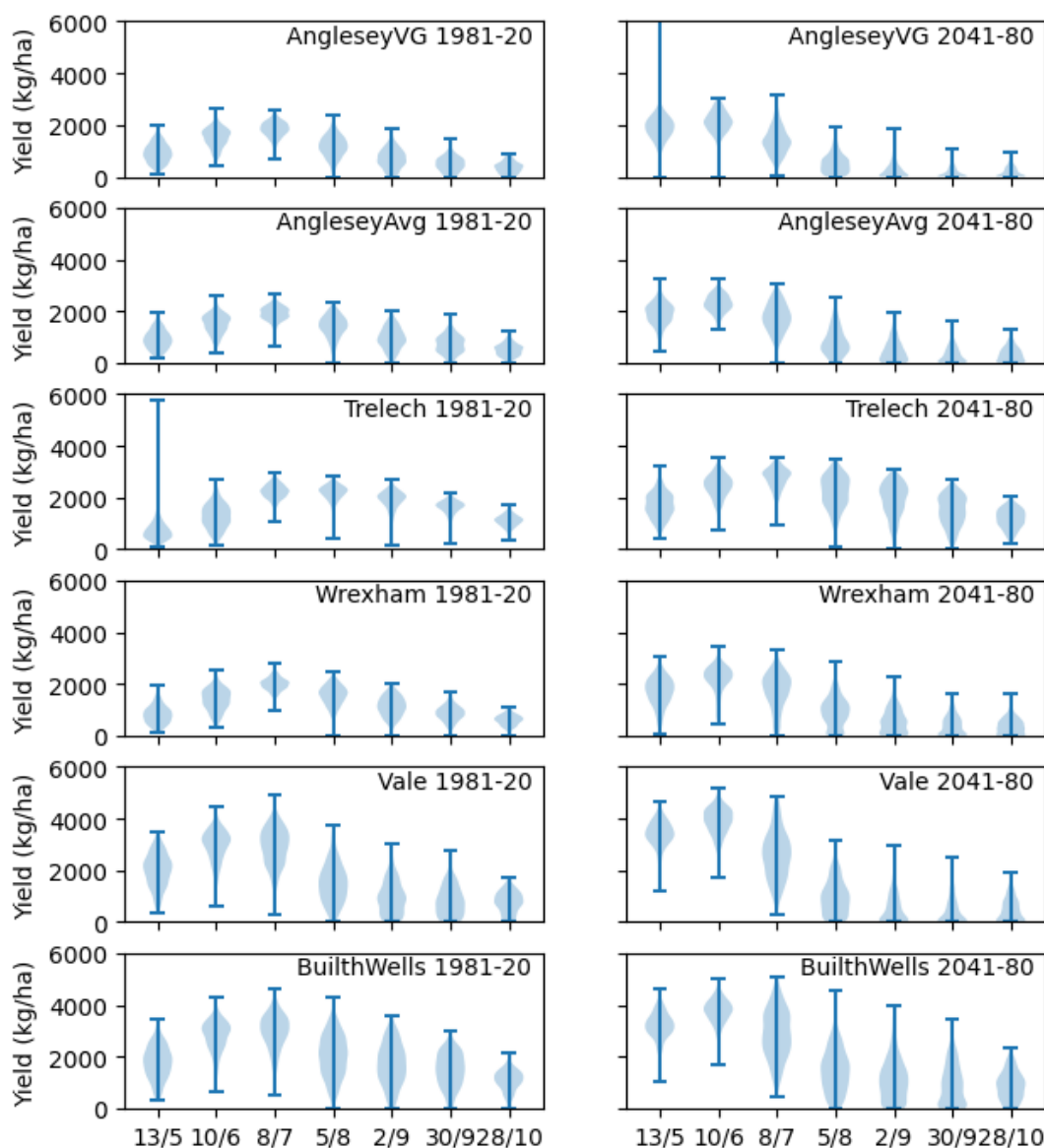


**Figure 3.6: Violin plots of simulated dry matter yields in each harvest at six study sites, for the 1981-2020 baseline window (left) and the 2041-2080 projection window (right) in the CO<sub>2</sub>-fertilised model. Bars represent the range of the data, and the shaded areas represent the shape of the distributions of the data for each harvest. Distributions comprise 40 individual years calculated across 12 model variants.**

There was no difference between the two CO<sub>2</sub> scenarios in fraction of the harvest taken before August (Figure 3.7), as the effect of CO<sub>2</sub> on dry matter yield was predicted to be proportional for each month.

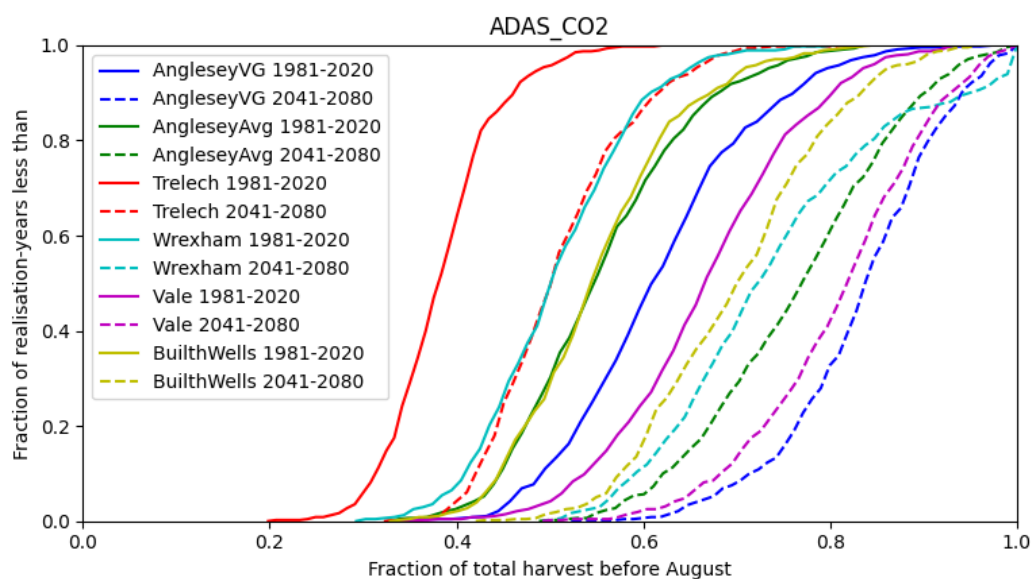


**Figure 3.7: Distributions of simulated fraction of total harvest pre-August at six study sites in both the 1981-2020 baseline (solid lines) and 2041-2080 projection (dashed lines) windows, under the CO<sub>2</sub> sensitive model. Distributions comprise 40 individual years calculated across 12 model variants. Curves are almost identical to those seen in the CO<sub>2</sub>-unfertilised case (Figure 3.4).**

## 4 DISCUSSION

### 4.1 Which sites prosper?

Consistently through the study, climate change was predicted to have the most positive impact on grass dry matter yields at the Trelech site. Examination of the seasonal yield patterns suggest that this is because the site was not predicted to experience significant yield reductions in August and later months, unlike the other sites. It is notable that Trelech currently has the highest annual average rainfall of all the sites, and its height above sea-level also makes it comparatively cool (Table 4.1). This is consistent with the functioning of the model – higher rainfall and lower peak temperatures in summer and autumn are predicted to provide good grass growth conditions throughout the season, with less impact from heat and drought.

**Table 4.1: Mean daily temperatures and rainfall amounts for each study site. Note the Trelech site is both the coolest and the wettest site.**

Site	Mean daily temperature 1981-2020 (deg C)	Mean daily temperature 2041-2080 (deg C)	Mean daily precipitation 1981-2020 (mm)	Mean daily precipitation 2041-2080 (mm)
AngleseyVG	10.7	13.5	2.1	1.7
AngleseyAvg	10.6	13.5	2.5	2.1
Trelech	9.3	11.9	5.1	4.7
Wrexham	9.7	12.4	2.5	1.8
Vale	11.2	13.5	2.8	2.8
BuilthWells	11.2	13.6	3.9	4.0

It might be expected that other localities in Wales experiencing similar conditions will respond similarly to climate change. This is somewhat encouraging, since the classification mapping (Figs. Figure 1.1, Figure 1.2) predicts these conditions fairly widely across inland, western and central Wales.

### 4.2 Consequences of changes to seasonality

This study suggests that in terms of total annual yields, many (though not all) locations in Wales will experience relatively small changes to total annual dry matter yields. However, the modelling suggests that there is likely to be a change to the seasonality of growth. The stability in total predicted yield in 2041-2080 compared to 1981-2020 was only achieved as a result of a significant predicted increase in early season growth that compensated for major to severe collapses in yields for late season harvests, with little grass growth predicted from August onwards.

The predicted changes in seasonality of grass growth are likely to have significant consequences for grazing management systems, as the lack of grass growth during the late summer period will reduce the length of the grazing season. In order to maximise the utilization of the predicted increase in early season growth it is likely that an increase in

silage making may be required to feed livestock during the periods of reduced grass growth. This is likely to require investment in farm infrastructure including buildings to house livestock and structures to store conserved grass. An increase in housed livestock will also increase the need to store and spread manures which will add costs to farm businesses. Silage-making can also change the nutritional content of feed: Wilkinson (2015) reports a decrease in metabolizable energy of ~24% between field and trough comparing silage to grass.

The late season collapse in dry matter yields was not predicted at all sites. The model predictions suggest that late season yield reductions may be relatively small at cooler and wetter farm sites, such as Trelech. The lack of imposed changes in management style forced by poor late season harvests may place a further premium on such sites, over and above the increases in total yields that such sites may receive.

### 4.3 Comparison with categorisation approach

Disabling the effects of increased atmospheric CO<sub>2</sub> concentrations in the AGM allowed direct comparison of the model predictions with the categorisation approach (Figs. Figure 1.1 Figure 1.2) based on AHDB Nutrient Management Guide (RB209) grass growth productivity guidelines (Table 4.2). In general, the model predictions qualitatively support the categorisation approach:

- Yield predictions for sites mapped as Good grass growth class under baseline (present) conditions have modelled yields significantly above those mapped as Average and Poor;
- The Trelech site, which the categorisation indicates will retain its Good growth class in 2080, was predicted to experience only a small, 3% fall in modelled total productivity;
- Sites forecast to fall in productivity class all experience greater than 10% reduction in modelled productivity.

**Table 4.2: Summary of key metrics comparing the RB209 categorisation mapping outputs with AGM outputs. Note that the rainfall classes presented here are drawn from the categorization mapping presented in Hockridge et al. (2020), and in some cases they differ to the bias-adjusted, mean modelled rainfall data used to drive the model (see Section 2.1.2).**

Site	Current productivity class	Projected productivity 2080	Soil type	Modern rainfall class	Modern water availability	Mean modelled rainfall 1981-2020 (mm/d)	Median yield, 1981-2020 (kg/ha)	Change w. CO <sub>2</sub> fert. (%)	Change, no CO <sub>2</sub> fert. (%)
AngleseyVG	Very good	Good	Silty clay loam	High	High	2.1	7,000	-8	-30
Trelech	Good	Good	Clay loam	High	Mid	5.1	11,000	24	-2
Vale of Glamorgan	Good	Average	Silty clay	High	Mid	2.8	11,900	3	-16
Builth Wells	Good	Poor	Clay loam	High	Mid	3.9	13,700	3	-17
Wrexham	Poor	Very poor	Sandy loam	Mid	Low	2.5	8,300	0	-23
AngleseyAvg	Average	Poor	Sandy loam	High	Low	2.5	8,000	-1	-24

Nevertheless, in detail there are some mismatches. Significant amounts of variability exist within each productivity class – which is to be expected given the broadness of the class approach – and there is some overlap between classes. For example, production at the Anglesey Average site was predicted as slightly lower than the Wrexham Poor site. Most obviously, however, predictions for the Anglesey Very Good site (AngleseyVG) gave surprising results, with predictions of low productivity under current climate and further declines in yields predicted by 2080. This difference is interpreted as reflecting a number of factors combining: (i) the classification places more weight on soil type in predicting dry matter yield than the model does, and the soil is classified as very good for growth at AngleseyVG; (ii) the site sits extremely low in the High rainfall category; (iii) the average of the time series of rainfall used in the modelling is notably lower than the average reported in the dataset used for the mapping.

These findings suggest that the categorisation approach is robust in how it describes relative changes in productivity around Wales as a result of changing weather patterns at wider spatial scales. However, at any given site, its predictions may be modified by specific and local variation in weather and soil type.

#### 4.4 CO<sub>2</sub> Fertilisation

Incorporation of CO<sub>2</sub> fertilisation into the AGM led to a c.20 percentage point increase in predicted yields. The increase was distributed proportionally throughout the year. As the model predicts greater dry matter yields in spring than summer, this CO<sub>2</sub> fertilisation effect translates into predictions of higher *absolute* dry matter production in spring.

However, as noted in the Methods, the CO<sub>2</sub> fertilisation model incorporated into the AGM is relatively simple. Although it mimics very closely the approach taken in other published models of grass crop growth (e.g., Romera et al., 2010), it nevertheless ignores or simplifies a number of physiological factors known to affect CO<sub>2</sub> promotion of growth. These include interactions with temperature, irradiance, water availability and humidity, leaf age, plant energy stores, transition to reproductive growth and flowering, nutrient availability, among other effects (e.g., Kaiser et al., 2015; Rodriguez et al., 1999). Some of these factors could potentially be incorporated into the model in a future iteration. Many of these factors act as limiters on the ideal biochemical processes of photosynthesis, and so we might anticipate that the AGM is giving somewhat optimistic estimates of CO<sub>2</sub> promotion of growth.

## 4.5 Further work

### 4.5.1 Climate change and management strategies

The modelling in this study has assumed that management strategies on the simulated crop will remain unchanged as climate change proceeds. In reality, there are numerous other factors that could be considered when assessing the impacts of climate change on grass productivity. These include:

- Changes in harvesting regimes (e.g., earlier starts to grazing)
- Nutrient application timing and rates
- Inherent improvements in crop productivity over time
- Reactive changes in grassland management in response to yield changes as they occur in the future (e.g. adoption of irrigation in late seasons)
- Changes to pastoral style (e.g., sheep to cows)
- Changes imposed by government policy
- Land use at regional scale:
  - conversion of tillage land to managed grassland
  - reduction in agricultural land area (including land use changes to achieve environmental benefits – biodiversity, reduction of agricultural pollution, etc.)
  - use of alternative crops, or changes to mixes of grass, herbal and legume species

Many of these changes will occur as a result of policy intervention, farm economic interests, and imposed environmental pressures. The modelling in this study could be adapted to incorporate a number of these management effects, which could be used to improve understanding of impacts of controls on land use as climate change proceeds.

### 4.5.2 Grass quality

The current iteration of the AGM estimates only the dry matter yield from a harvest. However, if grass is to be used to feed livestock, then the energy content and quality of that mass of grass is also important. One measure of this, the nitrogen content of ryegrass, can vary substantially, changing alongside growth rates, growth type (vegetative vs. reproductive), and harvesting regime, amongst other variables (e.g., Culleton et al., 1986). All of these parameters may be expected to change as climate change occurs, as documented here. Similarly, the fibre content of grass varies with, for instance, time in the year, with earlier, leafier harvests having lower fibre and higher nutritional content.

Future modelling based on that presented here could incorporate an assessment of grass quality alongside bulk yields. It is likely that the shift of growth into the early season predicted in this study will have significant, potentially positive, consequences for grass nutritional content.

### 4.5.3 Systematic uncertainties

This project has provided predictions of the impact of climate change on grass growth at six indicative sites across Wales. A more systematic approach that maps productivity across the country would provide a more in-depth understanding of the individual controlling factors (rainfall, wind, temperature, cloudiness, soil type, etc.). This would allow better estimates of

the impacts of weather changes at more local scales (e.g., for individual farms, and as national maps), and the calculation of confidence intervals and probabilistic projections.



## 5 REFERENCES

---

- AHDB (2021), *Nutrient Management Guide (RB209)*.
- Allen, R. G., Jensen, M. E., Wright, J. L., and Burman, R. D. (1989), 'Operational estimates of reference evapotranspiration', *Agronomy Journal*, 81/4: 650–662.
- Allen, R. G., Smith, M., Pereira, L. S., and Perrier, A. (1994), 'An update for the calculation of reference evapotranspiration', *ICID Bulletin*, 43/2: 35–92.
- Brereton, A., Danielov, S., and Scott, D. (1996), *Agrometeorology of grass and grasslands for middle latitudes. Technical Note 197* (Geneva, Switzerland: World Meteorological Organisation (839)).
- Brockman, J. (1995), 'Grassland', in J. Soffe (ed), *Primrose McConnell's The Agricultural Notebook* (19th ed.) (Oxford: Blackwell).
- Chang, J., Ciais, P., Viovy, N., Soussana, J.-F., Klumpp, K., and Sultan, B. (2017), 'Future productivity and phenology changes in European grasslands for different warming levels: implications for grassland management and carbon balance', *Carbon Balance and Management*, 12/11:.
- Christy, B., Tausz-Posch, S., Tausz, M., Richards, R., Rebetzke, G., Condon, A., McLean, T., Fitzgerald, G., Bourgault, M., and O'Leary, G. (2018), 'Benefits of increasing transpiration efficiency in wheat under elevated CO<sub>2</sub> for rainfed regions', *Global Change Biology*, 24/5: 1965–1977.
- Craig, J. (1984), 'Basic routines for the Casio computer', *Wayne Green Books, Peterborough, NH*, 3458: 131.
- Culleton, N., Fleming, G. A., and Murphy, W. E. (1986), 'A Preliminary Investigation into the Nitrogen Content of Three Cultivars of Perennial Ryegrass (*Lolium perenne* L.)', *Irish Journal of Agricultural Research*, 25/3: 307–312.
- Dellar, M., Topp, C. F. E., Banos, G., and Wall, E. (2018), 'A meta-analysis on the effects of climate change on the yield and quality of European pastures', *Agriculture, Ecosystems & Environment*, 265: 413–420.
- Department for Environment, Food & Rural Affairs (2020), *The British survey of fertiliser practice. Fertiliser use on farm crops for crop year 2019* (Fertiliser Manufacturers Association (FMA)).

- Department for Environment, Food & Rural Affairs, Department of Agriculture, Environment and Rural Affairs (Northern Ireland), Welsh Government, Knowledge and Analytical Services, and The Scottish Government, Rural and Environment Science and Analytical Services (2020), *Agriculture in the United Kingdom 2019* (National Statistics Service).
- Doyle, C., Ridout, M., Morrison, J., and Edwards, C. (1986), 'Predicting the response of perennial ryegrass to fertilizer nitrogen in relation to cutting interval, climate and soil', *Grass and Forage Science*, 41/4: 303–310.
- Duffie, J. A., and Beckman, W. A. (1980), 'Solar engineering of thermal processes', *NASA STI/Recon Technical Report A*, 81: 16591.
- Fung, F. (2018), *How to Bias Correct, UKCP18 Guidance, Met Office*.
- Gohar, L. K., Lowe, J. A., and Bernie, D. (2017), 'The Impact of Bias Correction and Model Selection on Passing Temperature Thresholds: Timings of Passing Warming Levels', *Journal of Geophysical Research: Atmospheres*, 122/22: 12,045-12,061.
- Hawkins, E., Fricker, T. E., Challinor, A. J., Ferro, C. A. T., Ho, C. K., and Osborne, T. M. (2013a), 'Increasing influence of heat stress on French maize yields from the 1960s to the 2030s', *Global Change Biology*, 19/3: 937–947.
- Hawkins, E., Osborne, T. M., Ho, C. K., and Challinor, A. J. (2013b), 'Calibration and bias correction of climate projections for crop modelling: An idealised case study over Europe', *Agricultural and Forest Meteorology*, 170: 19–31.
- Hess, T., Knox, J., Holman, I., and Sutcliffe, C. (2020), 'Resilience of Primary Food Production to a Changing Climate: On-Farm Responses to Water-Related Risks', *Water*, 12/8: 2155.
- Hockridge, B., Rollett, A. J., and Williams, J. R. (2020), *Grass Growth Classes, Report Code SPEP2020-21/01, Welsh Government (ADAS)*.
- Hollis, D., McCarthy, M., Kendon, M., Legg, T., and Simpson, I. (2019), 'HadUK-Grid—A new UK dataset of gridded climate observations', *Geoscience Data Journal*, 6/2: 151–159.
- IPCC (2014), *Climate Change 2014: Synthesis Report. Contribution of Working Groups I, II and III to the Fifth Assessment Report of the Intergovernmental Panel on Climate Change [Core Writing Team, R.K. Pachauri and L.A. Meyer (eds.)]* (Geneva, Switzerland: IPCC).

- Kaiser, E., Morales, A., Harbinson, J., Kromdijk, J., Heuvelink, E., and Marcelis, L. F. M. (2015), 'Dynamic photosynthesis in different environmental conditions', *Journal of Experimental Botany*, 66/9: 2415–2426.
- Laidlaw, A. S. (2009), 'The Effect of Soil Moisture Content on Leaf Extension Rate and Yield of Perennial Ryegrass', *Irish Journal of Agricultural and Food Research*, 48/1: 1–20.
- MAFF (1988), *Agricultural Land Classification of England and Wales: Revised guidelines and criteria for grading the quality of agricultural land* (London: Ministry of Agriculture Fisheries and Food).
- McCall, D. G., and Bishop-Hurley, G. J. (2003), 'A pasture growth model for use in a whole-farm dairy production model', *Agricultural Systems*, 76/3: 1183–1205.
- Met Office Hadley Centre (2018a), *UKCP18 Regional Climate Model Projections for the UK. Centre for Environmental Data Analysis, April 2021.*  
<http://catalogue.ceda.ac.uk/uuid/b4d24b3df3754b9d9028447eb3cd89c6>.
- Met Office Hadley Centre (2018b), *UKCP18 Regional Projections on a 12km grid over the UK for 1980-2080. Centre for Environmental Data Analysis, April 2021.*  
<https://catalogue.ceda.ac.uk/uuid/589211abeb844070a95d061c8cc7f604>.
- Met Office, Hollis, D., McCarthy, M., Kendon, M., Legg, T., and Simpson, I. (2018), *HadUK-Grid gridded and regional average climate observations for the UK. Centre for Environmental Data Analysis, April 2021.* <http://catalogue.ceda.ac.uk/uuid/4dc8450d889a491ebb20e724debe2dfb>.
- Met Office, Hollis, D., McCarthy, M., Kendon, M., Legg, T., and Simpson, I. (2020), 'HadUK-Grid Gridded Climate Observations on a 12km grid over the UK, v1.0.2.1 (1862-2019)', *Centre for Environmental Data Analysis*, 21 October 2020:
- Monteith, J. L. (1965), 'Evaporation and environment', *Symposia of the Society for Experimental Biology*, 19: 205–234.
- Monteith, J. L. (1981), 'Evaporation and surface temperature', *Quarterly Journal of the Royal Meteorological Society*, 107/451: 1–27.
- Morrison, J., Jackson, M. V., and Sparrow, P. E. (1980), *The response of perennial ryegrass to fertilizer nitrogen in relation to climate and soil. Report of the Joint ADAS/GRI Grassland Manuring Trial – GM 20. G.R.I Technical Report 27* (Hurley, Maidenhead, Berkshire, SL6 5LR).

- Neil, S. (2020), *June 2020 Survey of Agriculture and Horticulture: Results for Wales* (Welsh Government).
- Piani, C., Haerter, J. O., and Coppola, E. (2010), 'Statistical bias correction for daily precipitation in regional climate models over Europe', *Theoretical and Applied Climatology*, 99/1–2: 187–192.
- Rodriguez, D., Van Oijen, M., and Schapendonk, A. H. M. C. (1999), 'LINGRA-CC: a sink–source model to simulate the impact of climate change and management on grassland productivity', *New Phytologist*, 144: 359–368.
- Romera, A. J., Beukes, P., Clark, C., Clark, D., Levy, H., and Tait, A. (2010), 'Use of a pasture growth model to estimate herbage mass at a paddock scale and assist management on dairy farms', *Computers and Electronics in Agriculture*, 74/1: 66–72.
- Romera, A. J., McCall, D. G., Lee, J. M., and Agnusdei, M. G. (2009), 'Improving the McCall herbage growth model', *New Zealand Journal of Agricultural Research*, 52/4: 477–494.
- Schapendonk, A. H. C. M., Stol, W., van Kraalingen, D. W. G., and Bouman, B. A. M. (1998), 'LINGRA, a sink/source model to simulate grassland productivity in Europe', *European Journal of Agronomy*, 9/2–3: 87–100.
- Schwalm, C. R., Glendon, S., and Duffy, P. B. (2020), 'RCP8.5 tracks cumulative CO2 emissions', *Proceedings of the National Academy of Sciences*, 117/33: 19656–19657.
- Semenov, M. A. (2009), 'Impacts of climate change on wheat in England and Wales', *Journal of The Royal Society Interface*, 6/33: 343–350.
- Switanek, M. B., Troch, P. A., Castro, C. L., Leuprecht, A., Chang, H.-I., Mukherjee, R., and Demaria, E. M. C. (2017), 'Scaled distribution mapping: a bias correction method that preserves raw climate model projected changes', *Hydrology and Earth System Sciences*, 21/6: 2649–2666.
- Thomas, C., & Young, J. (Eds.) (1990), *Milk From Grass* (2nd ed.) (Billingham, Perth & Hurley: ICI, SAC, Grassland Research Institute).
- Watson, J., Challinor, A. J., Fricker, T. E., and Ferro, C. A. T. (2015), 'Comparing the effects of calibration and climate errors on a statistical crop model and a process-based crop model', *Climatic Change*, 18.

Whiteley, A., Willingham, L., Hockridge, B., Anthony, S., and Berry, P. (2018), *GRASS Improvement Using Satellite TECHNOLOGIES (GRASSS-TECH) Summary Report: Developing existing grass growth model to make use of remotely sensed data. ADAS report to AHDB (project reference 61100012).*

Wilkinson, J. M. (2015), 'Managing silage making to reduce losses', *Livestock*, 20/5: 280–286.

Wolf, J. (2006), *Grassland data from PASK study & Testing of LINGRA* (Wageningen: PPS).